Primary processes: from atoms to diatomic molecules and clusters

X. Fléchard, L. Adoui, G. Ban, P. Boduch, A. Cassimi, J.Y. Chesnel, D. Dominique Durand, F. Frémont, S. Guillous, J.P. Grandin, et al.

Primary processes: from atoms to diatomic molecules and clusters

2015 J. Phys.: Conf. Ser. 629 012001

(http://iopscience.iop.org/1742-6596/629/1/012001)

Journal of Physics: Conference Series **629** (2015) 012001 doi:10.1088/1742-6596/629/1/012001

Primary processes: from atoms to diatomic molecules and clusters

X Fléchard[1], L Adoui[2], G Ban[1], P Boduch[2], A Cassimi[2], J Y Chesnel[2], D Durand[1], F Frémont[2], S Guillous[2], J P Grandin[2], D Hennecart[2], E Jacquet[2], P Jardin[4], E Lamour[3], E Liénard[1], D Lelièvre[2], L Maunoury[4], A Méry[2], O Naviliat-Cuncic[1], C Prigent[3], J M Ramillon[2], J Rangama[2], J P Rozet[3], S Steydli[3], M Trassinelli[3] and D Vernhet[3]

[1] LPC Caen, ENSICAEN, Université de Caen, CNRS/IN2P3, Caen, France
[2] CIMAP, CEA - CNRS - ENSICAEN, BP 5133, F-14070, Caen cedex 5, France
[3] Institut des NanoSciences de Paris, CNRS, Sorbonne Université – Pierre et Marie Curie, UMR7588, 4 Place Jussieu, 75005 Paris, France
[4] GANIL, CEA/DSM-CNRS/IN2P3, F-14070 Caen, France

E-mail: flechard@lpccaen.in2p3.fr

Abstract. This article presents a short review of the main progresses achieved at the GANIL facilities during the last thirty years in the field of ion-atom and ion-diatomic molecule collisions. Thanks to the wide range of projectile energies and species available on the different beam lines of the facility, elementary processes such as electron capture, ionization and excitation have been extensively studied. Beside primary collision mechanisms, the relaxation processes of the collision partners after the collision have been another specific source of interest. Progresses on other fundamental processes such as Young type interferences induced by ion-molecule collisions or shake off ionization resulting from nuclear beta decay are also presented.

1. Introduction

For the electronic structures of atoms and molecules, precise theoretical knowledge and high-resolution experimental data are available. But the complete understanding of dynamic processes in atomic collisions remains a challenge, due to large theoretical problems in describing time-dependent many-particle reactions, and to experimental difficulties in performing complete experiments in which all relevant quantities are accessible. Elementary collisions involving ions, atoms and molecules play an important role in many gaseous and plasma environments, where they provide both the heating and cooling mechanisms. The study of such collisions is thus not only of fundamental importance, it is also essential for the understanding of large-scale systems such as astrophysical plasmas, planetary atmospheres, gas discharge lasers, semiconductor processing plasmas, and fusion plasmas. Collisions between ions and atoms (or simple molecules) give also access to the elementary processes responsible for energy transfer in ion-matter and ion-biological molecule collisions. Complete knowledge of these elementary processes is thus of primordial importance for ion induced modification of materials as well as for radiolysis, radiotherapy and biological damages due to radiation exposure.

For inelastic collisions involving energy exchange between the collision partners, three elementary processes can be distinguished: electron capture (or charge exchange), excitation, and ionization. The relative importance of these processes depends strongly on the collision regime that is linked not only to the projectile velocity, v_p, compared to the (classical) orbital velocity of the (active) target electron, v_e, but also to the collision asymmetry, i.e. the ratio Z_p/Z_t (Z_p and Z_t are the projectile and target atomic numbers, respectively). Therefore the collision strength parameter $K = (v_e/v_p)\times(Z_t/Z_p)$ defines the collision regime such as the strong interaction regime ($K>>1$) where electron capture is by far the most probable process, the perturbative regime ($K<<1$) where ionization and excitation dominate, and the intermediate regime ($K\cong 1$) where the three processes compete, leading to many collision channels, and in which both bound and continuum states have to be taken into account for the accurate calculation of the cross sections. Of course those collision regimes can be described in terms of collision energy only, provided $Z_p \geq Z_t$. The GANIL facility of Caen, France, has the very unique feature of covering most of the energy range of interest: the ARIBE experimental hall can provide ion beams from very low (a few eV/q) to low (25 keV/q) energy, IRRSUD delivers ion projectiles in the range of 0.1 to 1 MeV/A, and by using one or two of the main cyclotrons CSS1 and CSS2, energies from 4 to 100 MeV/A are accessible. In addition, the SPIRAL1 target-ion source assembly provides low energy radioactive ions, making available the study of the electron cloud rearrangement following nuclear reactions. The GANIL is thus, for more than thirty years, a privileged experimental center to study dynamic processes with atomic and molecular targets.

The goal of the present article is to list the main advances in the field achieved thanks to the GANIL beams and to the CIMAP through the CIRIL user facility. The first section will be dedicated to experiments using atomic targets and the second section will present results obtained with small molecules and rare gas dimers. In the last section we will also discuss other fundamental dynamical processes involving ions, atoms and molecules, in which collision is the tool to reveal specific effects. The reader should be warned that this article is not an exhaustive review of ion-atom and ion-molecule collisions, what would be well beyond the scope of the present work. It is only focused on experiments performed at GANIL in the domain, with different techniques, and different specific scientific motivations that are not always naturally linked to each other.

2. Achievements in ion-atom collisions

2.1. In the strong interaction regime

Charge exchange in low-energy ion-atom collisions has been extensively studied for decades. Concurrent advances in experimental and theoretical techniques have led to a satisfying knowledge of the underlying dynamics, which is reviewed in textbooks such as [1]. However, the interest in this fundamental process has never faded out since charge exchange plays an important role in astrophysical and Tokamak plasma environments [2, 3], ion-induced radiation damage to biological cells [4, 5], and many other current applications.

2.1.1. Single electron capture.

- *Photon spectroscopy experiments*

Single electron capture leads to the population of excited states $n\ell$ of the scattered projectile ions. These excited states are below the first ionization limit of the scattered ion, thus leading to its decay by photon emission. The detection of photons emitted by the projectile and the measurement of their energy carry information on both, the spectroscopy of the resulting scattered ion, and the capture process itself.

The populated energy levels n depend mainly on the charge of the projectile and on the target ionization potential [6]. For this process, the photon spectroscopy in the range 200-600 nm is a good tool to observe Δn=1 and Δn=2 transitions [7, 8]. With the help of Hartree Fock calculations [9], it is then possible to get spectroscopic information about the energy structure of the ions produced during the collision. In the particular case of the Ar^{8+} ($1s^2 2s^2 2p^6$), a large set of targets has been used : He, H_2,

Li, Cs(6s) and Cs(6p) leading to the population of Ar VIII ($1s^2 2s^2 2p^6 n\ell$) with n=4 to 14 [8-12]. For this Ar VIII ion, many new energy levels and fine structure values have been determined [8].

Photon spectroscopy in the 200-800 nm is powerful enough to observe lines from each $n\ell$ configuration inside a same n level. The emission cross sections have been determined from the line intensities and the spectroscopic response of the optical system. The production cross sections for each $n\ell$ populated level can then be determined from the emission cross sections and the branching ratios of the emission levels in order to take into account the cascade effects on the populated levels. An example is shown in figure 1 for the Ar^{8+}-Li(2s) collision [13]. It was shown that the final $n\ell$ distributions are not statistically distributed: states with large ℓ values are strongly populated, but also states with low ℓ values (ℓ = 0, 1, 2). In most cases, the experimental production cross sections are in fair agreement with those obtained using the Classical trajectory Monte Carlo (CTMC) method (figure 1) [13-15].

At GANIL, special attention was focused on the projectile energy dependence of the production cross sections: for states with large angular momenta, no dependence has been observed, but, for a given n state (n = 8, 9 and ℓ = 0, 1, 2), the $n\ell$ cross sections increase with decreasing projectile energy. These results have then been analyzed in terms of dynamical couplings by using calculations of the electronic energies of the one-electron $(Ar^{7+}\text{-}Li)^+$ system. The $n\ell$ distributions result from both the primary capture process and the post-collisional effects: these two processes depend not only on the relative importance of the radial and rotational couplings but also on the Stark mixing and on the projectile–core-electron effect. In the case of fully stripped ions colliding with lithium atoms (O^{8+}–Li), all $n\ell$ sublevels (n fixed) are affected by the Stark effect due to the Li^+ residual ion. The population of states with large ℓ values is then favored and only states with large ℓ values are populated by single-electron capture. In the case of Ar^{8+}–Li collisions, the presence of the projectile core electrons lifts the degeneracy of the $Ar^{7+}(n\ell)$ states with low ℓ values (ℓ<4) and only the states with high ℓ values are affected by the Stark effect. The $n\ell$ cross sections for ℓ<4 are strongly affected by the core-electron effect at low energy. It leads to the enhancement of the population of states with low ℓ values. The evolution of the $n\ell$ distributions with the projectile velocity depends on the evolution of the dynamical couplings: the effect of the projectile core electrons vanishes at high energies [16, 17].

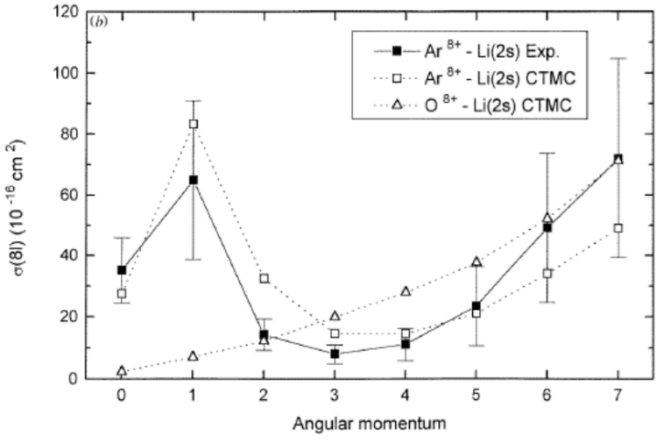

Figure 1. 8ℓ-distribution for X^{8+}-Li(2s) (X = Ar, O) collisions (projectile energy of 0.5 keV.amu^{-1}) [13].

In order to determine the m distributions, the polarization P of the emitted light has been measured. The polarization of a transition can be calculated from m capture cross sections into the different m Zeeman sublevels of the $n\ell$ upper level, taking the ion beam direction as the quantization

axis. Since the spin-orbit coupling is negligible for transitions from levels such as $\ell > 2$, the formalism of Fano and Macek [18] was used. Calculated polarization ratios were obtained from these CTMC Zeeman sublevel populations. In order to make a correct comparison between the calculated and the experimental results, polarization calculations including radiative cascade effects were performed by using the method of Lin and Macek [19]. For the 8ℓ-9ℓ' transition for the Ar^{8+}-Li system, the high positive polarization degrees measured at the highest and lowest energies indicate that sublevels with $m = 0$ are preferentially populated. The decrease of the polarization with the collision energy indicates a broadening of the *m*-distributions, which is also obtained in the CTMC distributions. It is well established that the evolution of the *m*-distributions reflects the energy dependence of the couplings involved in the collision [20]. In the present case, the radial and rotational couplings, combined with the projectile–core electron effect and the Stark effect of the ionized target are responsible for the final $n\ell m$-distributions.

- *Kinematically complete experiments*

In the 1990s, the development of the COLTRIMS (Cold Target Recoil Ion Momentum Spectroscopy) technique [21-23], developed in parallel in Frankfurt (Germany), Manhattan (Kansas, USA) and Caen (France), provided new means to study charge exchange processes in low energy collisions. By giving access to both the Q-value and projectile scattering angle through the recoil ion momentum measurement, this technique is particularly well suited to perform kinematically complete experiments. In contrast with energy gain spectroscopy [24], the resolution in Q-value and scattering angle is not limited by the transverse emittance and by the energy dispersion of the projectile beam. In addition, the recoil ions are collected using an electric field that can be conveniently adjusted to insure 4π–detection efficiency. Combined with the high performances of the GANIL ECR source, the high detection efficiency of the COLTRIMS technique provided adequate conditions to study collisions involving fully stripped highly charged ions with charge states above 8+. The measurement of the final *n*-state dependence of the captured electron in coincidence with the associated scattering angle distributions could, for the first time, be performed in collision systems such as Ar^{18+} + He at 270 keV and Ne^{10+} + He at 150 keV. These challenging experiments provided new information about the reaction window and impact parameter dependence in single capture processes, and were used to test theoretical calculations based on the CTMC and the COBM (Classical Over the Barrier Model) methods. The measured *n*-state distributions were found to be in good agreement with both, the results of the CTMC calculations, and the $q^{0.75}$ dependence predicted by the COBM [25, 26]. Soon after, improvements of the experimental technique, such as the implementation of an inhomogeneous electric field for recoil ion collection, allowed to achieve even higher resolution on the recoil ion momentum measurement. By resolving the structures of the projectile scattering angle distributions, information about possible interferences between the different capture pathways (Stuckelberg oscillations) became available. This detailed information allowed to perform more stringent tests of close-coupling calculations using pseudo empirical exchange interaction for C^{5+} + He collisions at energies ranging from 9 keV to 90 keV [27]. In particular, the oscillations in scattering angle predicted by the calculation for 30 keV collisions were clearly observed in the experimental data. For Ne^{10+} + He collisions at 50 keV and 150 keV, the experimental scattering angle distributions obtained in the single capture process led to the validation of state-of-the-art close-coupling calculations including double capture channels and using wave functions based one-electron diatomic electron orbitals (OEDM) [28]. This constituted an important step in preparing detailed studies of the double electron capture processes. If the COLTRIMS technique proved to be a powerful tool to understand in more details the single electron capture process, it also provided new and valuable experimental results in the case of multiple electron capture, as shown in the next sections.

2.1.2. Double electron capture. When a highly charged ion collides an atomic He target at low projectile velocity ($v < 1$ a.u.), the ion may capture one or two electrons from He. Even in the case of collisions involving only two active electrons, the processes responsible for double electron capture

(DEC) were under debate during more than ten years [28-50]. Attempts to describe DEC by using independent electron models were not fully satisfactory. It has been shown that dynamic correlation effects due to the electron-electron interaction – which is not incorporated in these models – may play a decisive role during the collision [40-45]. The importance of these processes was found to depend strongly on the collision system and the projectile velocity.

DEC leads to the population of doubly excited states of the projectile ion. The production of quasi-equivalent (QE) electron configurations and non-equivalent (NE) electron configurations was investigated experimentally by means of Auger electron spectroscopy, in the case of C^{6+}, N^{7+}, O^{8+} and Ne^{10+} + He collisions [28,38-49]. At relatively high projectile velocities (~ 0.5 a.u.), QE configurations are mainly populated. This can be explained by using independent electron models. A first electron is captured and, independently of this electron, the second one is then captured. Here, electron-nucleus interaction is the main interaction responsible for such a capture. However, NE configurations are also populated, in a less extent, due to electron-electron interaction during the collision. As the projectile velocity decreases, the population of NE configurations strongly increases, showing that electron-electron interaction can play a decisive role during DEC. To identify more precisely the mechanisms responsible for the population of non-equivalent electron configurations, close-coupling calculations of DEC differential cross sections were performed and compared with experimental distributions [28, 41]. These calculations were useful to reveal the importance of the electron-electron interaction. Cold Target Recoil ion momentum spectroscopy (COLTRIMS) was also used to study the different mechanisms responsible for DEC [28, 49]. As an example, differential and doubly-differential cross sections for single-electron capture onto the levels n = 3,4,5 and 6 of $Ne^{9+}(nl)$ and double-electron capture onto series of doubly excited states 3,n and 4,n with n = 4, 5 and 6 of Ne^{8+} were obtained (figure 2) [28].

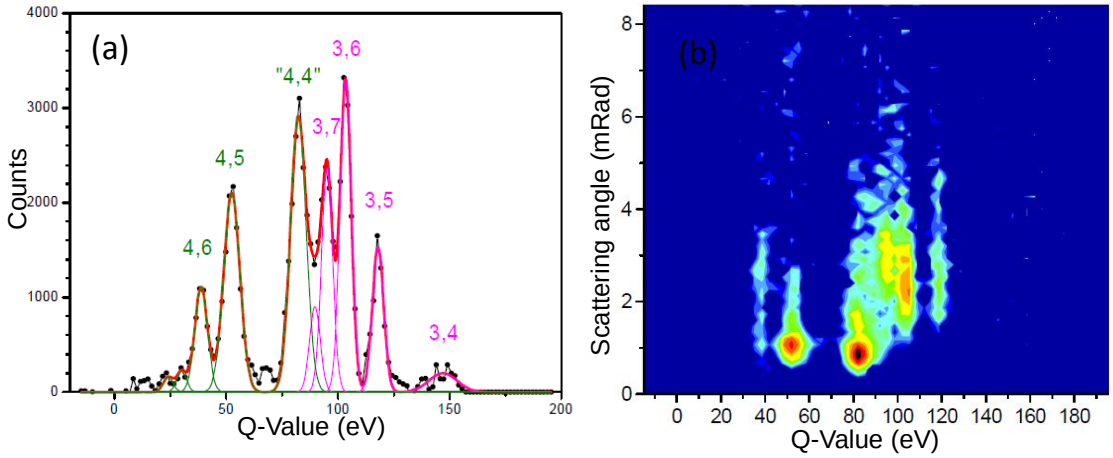

Figure 2. Cross sections differential in Q-Value (a) and doubly-differential in Q-Value and scattering angle (b) for the double electron capture process in Ne^{10+} + He collisions at 50 keV [28].

The cross sections were found to be in good agreement with state-of-the-art close-coupling calculations based on the use of OEDM orbitals. Population mechanisms for the dominantly populated double-capture channels could be deduced. In particular, it was found that even configurations of QE electrons can be populated by electron-electron interaction [28]. The population of NE electron configurations and its dependence on the collision velocity can also be attributed to post-collisional processes. These processes imply a population transfer from QE electron configurations, populated in the primary collision process, towards NE electron configurations with similar energy levels [51, 52]. The relative contribution of such processes and of the electron-electron interaction could be estimated thanks to this joint experimental/theoretical investigation. In addition, the extensive study of DEC

from He made possible to derive scaling laws for electron capture in A^{q+} + He collisions at low impact velocities [45].

Finally, *K*-shell vacancy production due to dielectronic excitation has been studied in order to give direct experimental evidence for electron correlation [53,54]. The study has been performed for collisions between bare N^{7+} ions and Ne atoms. Projectile velocities ranging from 0.1 to 0.7 a.u. were investigated. The method of Auger electron spectroscopy was used to measure cross sections for producing a *K*-shell vacancy in the multi-electron target of Ne. At the low impact velocities investigated here, the cross sections were shown to be of the order of 10^{-17} cm^2. Since single excitation or ionization plays a negligible role at velocities as low as a few tenths of an atomic unit, dielectronic excitation governed by the electron-electron interaction was shown to be the unique mechanism that is responsible for the production of *K*-shell vacancies in the present collisions. The remarkable feature is that the process of dielectronic excitation is likely enough to give rise to relatively large cross sections for producing *K*-shell vacancies in very slow ion-atom collisions. Moreover, it was shown that the transfer of spectator electrons creates resonance conditions for the transfer of two active electrons via dielectronic excitation. It has been found that dielectronic excitation is particularly favored when 3 target electrons are transferred into an excited state of the projectile [54].

2.1.3. Multiple electron capture with heavy targets. Starting from the 1980s, many experiments have been performed with light ions, like C, N, Ne interacting with light targets as H_2 and He. As illustrated above, using different techniques, they lead to a quite complete understanding of the mechanisms involved in the collision [55-61]. At the same time, extended theoretical investigations have been developed. They include simple approaches such as the well-known classical over-the-barrier model (COB) [62] or the reaction window within the Landau–Zener model [63, 64], and more sophisticated coupled state calculations using basis of either atomic or molecular orbitals [65-68].

However, today, there is still a lack of data for (quasi)symmetric collisions, i.e. highly charged ions colliding on many-electron targets whilst it is indeed one of the most common fundamental processes in space such as for instance when solar wind collides with comets. Until now, the only systematic studies available are restricted to coincidence measurements between charge selected projectile and target ions [69,70] where stabilized charge exchange mechanisms are investigated.

2.1.4. Using COLTRIMS. A preliminary study of multiple capture processes in low energy (105 keV) N^{7+} + Ne collision was also attempted using the COLTRIMS technique [71]. The resolution in Q-value that can be achieved with this technique cannot compete with high resolution electron spectroscopy or photon spectroscopy, but the measurement in coincidence of the charge states of both the projectile and the recoil ion gives direct access to capture multiplicity and to the stabilization ratios of the captured electrons. In this experiment, the branching ratios for configurations populated by the single and double capture processes could be clearly resolved and quantified. For the capture of three, four and five electrons, the populated configurations could be identified but the associated branching ratios could not be accurately determined. However, it was clearly shown that triple-, quadruple-, and quintuple-electron capture populate double Rydberg states and prefer to be doubly stabilized, with two electrons remaining on the scattered projectile while the others are ejected by Auger emission. With more than two active electrons, the number of channels leading to multiple capture becomes too large to be treated theoretically within the quasimolecular description and using close coupling standard calculations. Only the COBM [63] and a semi empirical model [72] could be used to describe these processes and be compared with the experimental results. These models predict a triple-electron capture stronger than the quadruple-electron capture, what was found to be in complete disagreement with the experimental results. This implies that electon-electron interaction, not included in these oversimplified calculations, may play an important role in multiple capture.

2.1.5. What can be learned from high-resolution x-ray spectra on low energy collisions for (quasi) symmetric heavy systems? Using low-resolution x-ray detection technique, experiments have been

performed [73-76], allowing to extract a parameter called the 'hardness ratio', H, (i.e. the ratio between the x-ray intensity of $n > 2 \rightarrow 1$ and $2 \rightarrow 1$ transitions) that serves as a reference to diagnose the relative abundance of constituents of intergalactic clouds and comets when interpreting astrophysical x-ray spectra [77,78]. Nevertheless, neither from ion charge state coincidence measurements nor from low-resolution x-ray spectroscopy, information on the partial $n\ell$ electron capture states is accessible. Furthermore, in the case of low-resolution x-ray measurements, as discussed recently in [79], the effect of single and multiple processes cannot be distinguished.

Of course, if a highly charged projectile collides with a many-electron target, multiple capture is possible and multiply excited projectile states can be formed. This gives rise to a complex de-excitation cascade that involves both Auger and radiative transitions. Unless one would do a "complete experiment" that measures all relevant photon and ion charge state coincidences (and possibly Auger electrons as well) it is difficult to obtain complete information on such a collision system from measurements alone. Similarly, the predictive power of theoretical calculations is limited simply because a full first-principles calculation of the many-electron dynamics is not feasible.

In a recent experiment performed at the low energy installation ARIBE at GANIL, the contribution of single-electron capture has been successfully disentangled from multiple-capture processes in the x-ray emission of an Ar projectile colliding with a N or Ar gaseous target at $v = 0.53$ a.u. [80]. By combining low-resolution spectroscopy, using Silicon Drift Detectors (SDD) but accurately calibrated in efficiency, with a complete determination of the ion beam-gas target overlap, absolute x-ray emission cross section has been extracted: a value of 11.4×10^{-15} cm^2 ±15 % has been found, in agreement with the only previous measurement performed by Tawara et *al*. [74] but with an improvement by more than a factor of 2 in the uncertainty and without referring to any external calibration.

Going a step further and taking full advantages of the high resolving power of a mosaic crystal spectrometer, additional information on single- and multi-electron processes have been achieved without applying coincidence with target charge-state detection. The whole He-like Ar Lyman series from $n = 2$ to 10 has been resolved as well as the fine structure of $n = 2 \rightarrow 1$ transitions (see figure 3) [80]. For each n value, the relative $1snp \rightarrow 1s^2$ intensity is obtained showing that the $1s2p \rightarrow 1s^2$ transition represents almost 90% of the total x-ray emission whatever the gaseous target (Ar or N). Resolving also the different $1s2\ell \rightarrow 1s$ transitions allows for a precise determination of the influence of metastable states such as the $1s2s\ ^3S_1$ state. It emphasizes that transposition of the commonly used hardness ratio, H, measured via 'laboratory ion-atom collisions' towards interpretation of spectra from comets and solar winds should be made with caution. Here, having control on the contamination from metastable Ar^{16+} ions in the incoming ion beam, an H value of 0.060 ± 0.007 has been found, approaching to the statistical limit as expected at a collision velocity of 0.53 a.u..

From the analysis of the $n = 7-10 \rightarrow 1$ line intensities, single-electron capture is found to occur preferentially in $n = 8–9$ with a relative n-distribution $\{Pn\}$ in agreement with the well-known Landau-Zener model [64]. In particular, $\{Pn\}$ is found to be independent on the ℓ-sublevel distribution population $\{P\ell\}$. The accurate knowledge of the Bragg-spectrometer transmission enables also to evaluate the absolute value of the single-electron capture cross section. In this case, the result is influenced by the choice of $\{P\ell\}$ and lies between $\sigma_{single} = 4.6\ 10^{-15}$ cm^2 (flat distribution) and $12.8\ 10^{-15}$ cm^2 (statistical distribution). This result can be satisfactorily compared to the value of about $8\ 10^{-15}$ cm^2 obtained by Ali *et al* [70] from coincidence measurements of projectile–target charge exchange for Ar^{17+}on Ar at $v = 0.6$ a.u., and is, as well, in good agreement with the classical over-barrier model [63].

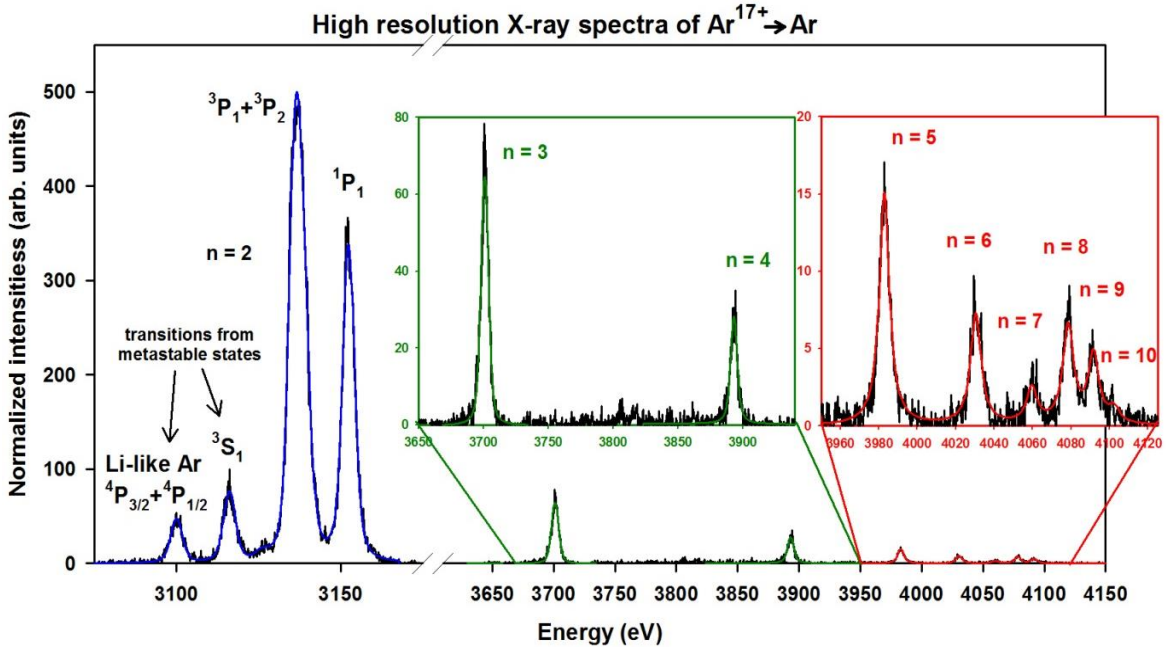

Figure 3. High-resolution spectra of Ar^{16+}x-ray transitions observed with an argon target in single collision condition. The He-like Ar 1s*n*p→ $1s^2$ with n up to 10 are visible. For $n = 2$, transitions from 1s2p $^3P_1$,$^3P_2$,$^1P_1$ to the ground level are partially resolved. In addition, M1 1s2s $^3S_1 \rightarrow 1s^2{}^1S_0$ and Li-like Ar 1s2s2p $^4P_{1/2,3/2} \rightarrow 1s^2 2s\ ^2S_{1/2}$ transitions are observed and well resolved from the 1s2p He-like transitions [80].

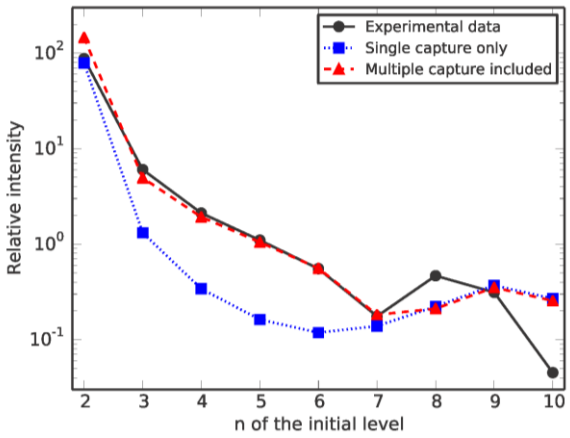

Figure 4. Experimental and calculated x-ray intensities for 1snp → $1s^2$ transitions in Ar^{16+} following capture in Ar^{17+}-Ar collisions at 0.53 a.u.

With the knowledge of $\{Pn\}$, the multi-electron capture contribution can also be estimated through the comparison between the experimental data and the expected intensities of the $n = 2 - 6 \rightarrow 1$ lines from single-electron capture using a cascade code. Those findings initiated new theoretical developments based on a two-center basis generator method (TC-BGM), in the independent electron model approximation, but including projectile states up to the 10^{th} shell in the basis [81]. They confirm that levels of $n \geq 7$ are populated only by single-capture (see figure 4), although at variance with experimental data for n=8 and 10 that is possibly due to the limited basis set used in the TG-BGM calculations. Besides, the theoretical results that include the multiple capture contributions are in very good agreement with the experimental data, while those which ignore them yield considerably lower

intensities [82]. This demonstrates quite clearly the important role of the multiple capture processes in this type of collision systems and allows even quantifying its influence.

2.2. In the perturbative regime

For electron transitions occurring in fast ion-atom collisions, where the projectile velocity is much greater than the velocity of the active bound electron, the collision interaction is weak so that perturbative methods can be used to treat the collision dynamics [83]. The emission of slow electrons in soft collisions at large impact parameter is usually attributed to three-body effects between the projectile, the electron, and the target ion. On the other hand, for larger momentum transfer, two-body interactions involving binary-encounter processes become important. The two- and three-body processes are analogous to Compton scattering and photo-absorption, respectively. Because of their similarity to photon induced interactions, excitation and ionization by ions traveling near relativistic speeds ($v \sim 100$ a.u.) are expected to occur mainly by dipole ($\Delta l=1$) transitions. Due to the uncertainty principle $\Delta l.\Delta\theta = 1$ (θ is the emission angle relative to the beam direction), the angular momentum transfer affects the angular distribution of the emitted electrons. Low-order multipole transitions produce a broad angular distribution and vice versa.

In addition to single electron transitions, excitation and ionization can be part of a multi-electron transition. In fast ion-atom collisions, two-electron transitions can be caused by separate nucleus-electron *(n-e)* interactions, or by an *n-e* interaction followed by an electron-electron (*e-e*) interaction (e.g. reference [84] and references therein). In the former case, the process is referred to as TS2 (two-step with two projectile interactions), and in the latter case it is called TS1 (two-step with one projectile interaction). The TS1 process implies dynamic electron correlation which generally falls into two categories, corresponding to whether the first electron is emitted slowly or suddenly. For slow emission, subsequent excitation or ionization of a second electron involves the mutual scattering of two electrons, i.e., it is *dielectronic* in nature. On the other hand, sudden emission can result in a subsequent electron transition due to the change in potential seen by the second active electron as the excited system relaxes [85]. This latter type of transition is a "mean-field" effect referred to as a *shake* process.

During the past decades, ionization and excitation of helium by fast ions and photons have attracted much interest (see e.g. [86]) due to the insight it provides into dynamic correlation effects. At CIRIL, we mostly focused on the ionization and excitation of the three-electron atom of lithium. In contrast to He in which initial-state correlation is strong (both electrons initially occupy the same orbital), the Li atom has the advantage that, for double ionization, initial-state correlation is small. Furthermore, an important reason for investigating excitation in Li is the fact that both single- and double-*K*-shell vacancy production can be measured in the same experiment via Auger-electron emission (this is not possible for He).

As a first step, we investigated the cross-section ratio for double-to-single ionization for collisions of 95-MeV/u N^{7+} with He and Li target atoms [87]. The measured values for Li and He were found to be about equal (~ 0.3 %). Double ionization of He is dominated by *e-e* interactions such as shake-off and initial-state correlation. On the other hand, though double ionization of Li is dominated by *n-e* interactions (TS2), the contribution of the shake-off process is not negligible. After removal of one of the 1*s* electrons of Li, the probability for shake-off is ~ 0.38 % for the ejection of either the 1*s* or 2*s* electron [87].

Besides total cross sections, we measured doubly differential cross sections for single ionization in collisions of 95 MeV/u Ar^{18+} with atomic Li for electron emission energies ranging from 3 to 1000 eV and emission angles ranging from 25° to 155° relative to the beam direction [88-90]. The high projectile velocity provided by the GANIL facility made possible the separation of two- and three-body processes in both angular and energy distributions of the ejected electrons. Emission of the 1*s* electron was shown to be mainly influenced by three-body effects [88]. The cross section for three-body collisions rapidly decreases with the electronic energy transfer so that two-body effects dominate at high electron emission energies [88,89]. Remarkably large contributions from two-body collisions

were also observed for the low-energy emission of the 2*s* electrons [89,90]. We moreover demonstrated that the node in the Li 2*s* wave function manifests itself in the angular spectra [88,90].

In parallel to ionization process studies, we devoted much attention to single and double excitation, as well as to excitation plus ionization processes. We investigated single-*K*-shell excitation and double-*K*-shell vacancy production in lithium by 95-MeV/u Ar^{18+} [91-93] and 60-MeV/u Kr^{34+} impact [94]. To separate TS1 and TS2 contributions, it was useful to vary the projectile charge-over-velocity ratio, q/v, since transition amplitudes for TS1 and shake depend linearly on q/v, whereas the transition amplitude for TS2 depends on $(q/v)^2$ [95]. Single-*K*-shell excitation was found to take place essentially by dipole transitions, leading to the excited states $1s2snp\ ^2P$. However, in the case of double *K*-shell-vacancy production, monopole transitions play a significant role, providing evidence for the *e-e* interaction. High-resolution Auger electron spectra showed that discrete doubly vacant *K*-shell states are predominantly formed from ionization plus excitation, giving rise to the $2sns\ ^{1,3}S$ and $2snp\ ^{1,3}P$ states of Li^+. The shake-up and dielectronic manifestations of the electron-electron interaction were shown to be the only mechanisms for creating the observed $2sns\ ^{1,3}S$ states. For $q/v < 2$ a.u. the formation of the $2snp\ ^{1,3}P$ states was found to be mediated only by the dielectronic process, permitting this aspect of the electron-electron interaction to be separately identified and its contribution characterized for the first time [93-96].

At high energy, for which the perturbative regime is reached, the high resolution measurements allowed by the COLTRIMS technique have led to experiments for testing the available theories on the few-body problem of the spatial and temporal evolution of mutually interacting particles. One of the most commented results has been obtained on the LISE beam line of GANIL by a collaboration between MPIK, Heidelberg and CIMAP. It was devoted to single and double ionization of He by 100 MeV/u C^{6+}. GANIL was the only place in the world to perform this experiment thanks to the available beam intensities but also to the fast bunch suppressor which could provide 1 ns ion bunches every 2 µs. Unique experimental results have been obtained concerning the double ionization [97], but surprising results on single ionization [98] have led to a 10-year-lasting discussion about the disagreement between experiment and theory (figure 5). This controversy is still open and new experiments are planned at GANIL to give a final and satisfactory answer to this disagreement.

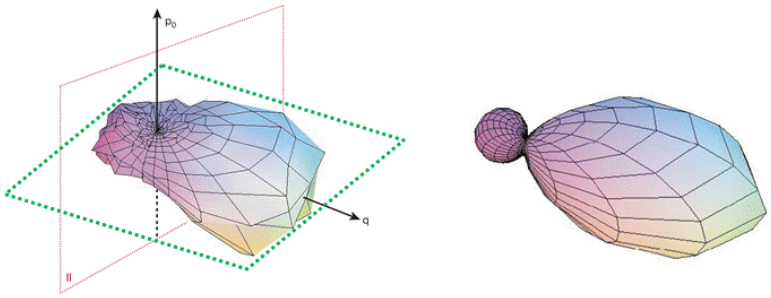

Figure 5. Electron angular distribution of helium single ionization induced by 100 MeV/u C^{6+} [99] for fixed momentum transfer q (q=0.75 u.a.) and electron kinetic energy (E=6.5 eV). Experimental results on the left, 3DW-theory on the right side.

2.3. In the intermediate regime

While significant progresses have been achieved when the perturbation induced by the target-atom is either very low or very high, as described above for instance, the full description of the dynamics of ions colliding with neutral targets in the so-named intermediate regime (i.e. K≅1, as defined in the introduction of this paper) is still lacking. Indeed, for this domain, cross sections of single-electron processes (capture, ionization or excitation) are of the same order of magnitude and interferences between all these channels cannot be neglected [100,101]. On the other hand, the role of target electrons as active partners, via capture-channel coupling and direct target electron – projectile electron interaction is not well known despite several attempts for a few specific cases (see for instance [102-105] and even recently [106,107]). The theoretical description of such many-electron systems is very complex and up to now these effects are not well taken into account even by the most

sophisticated approaches. Furthermore, multiple processes, involving more than one electron of the projectile and of the target as well, start to play a role and raise much debate question even today. Experimentally, disentangling the different channels involved is also a challenge [108,109] and this collision regime remains to be explored in details whereas it corresponds to the collision domain of major interest for applications since the ion stopping power is maximum.

Performing an experiment on the medium energy line (SME; Sortie Moyenne Energie) at GANIL, with high intensity beam of Ar^{16+} at a fixed velocity, v_p= 23 a.u. (13.6 MeV/u), but using gaseous neutral targets from He to Xe, the whole range from the perturbative regime to the strong interaction regime was able to be spanned. In addition, taking full advantage of the spin selectivity in the population of the projectile excited states via the different processes involved, the single-capture (SE), filling only singlet states from the fundamental heliumlike Ar^{16+} state $^1S_0$, has been fully distinguished from the capture-ionization (CI) process, which populates triplet states as well. The same argument holds for double-excitation (DE) versus capture-excitation-ionization (CEI). Of course this type of measurements requires resolving the different final-state configurations that are separated only by a few eV. By using a high-resolution and high-transmission spectrometer, specifically designed for this experiment, cross sections of all the different processes mentioned above have been determined, including the excitation-ionization (EI) which produces hydrogenlike Ar excited states [110].

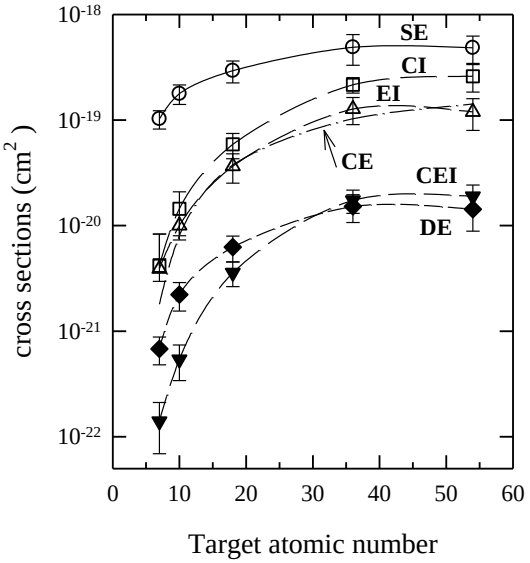

Figure 6. Single and multiple processes cross sections in n=2 for $Ar^{16+}\rightarrow Z_t$ collisions at v_p= 23 a.u. (13.6 MeV/u)

As shown in figure 6, all the processes, including both target-electrons – via capture channels – and projectile ones increase more rapidly than those involving only projectile electrons: CI for instance, which is negligible for He target (i.e. in the perturbative regime) reaches 54% of SE for Xe (i.e. when hitting the strong interaction regime). Nowadays, none of the available (even the most sophisticated) theories are able to reproduce those results on the full range of dynamics investigated here, although significant developments have been made. Only scaling laws reproducing the general relative behavior of the multiple processes compared to SE have been extracted [111, 112]. It is also worth mentioning that, even if the observed saturation of the "pure" single-excitation process, when the perturbation induced by the target-atom increases, is well predicted by the most recent models, disagreement by almost a factor of 2 was revealed starting from symmetric collisions [110]. This variance has been assigned to the role of the target-electrons, like the so-called anti-screening effect (direct projectile electron – target electron interaction), and the interferences with the capture channels which increases for high Z_t. More generally, those results demonstrated the crucial role of target

electrons when an ion interacts with neutral matter in the intermediate collision regime, which undeniably deserves further detailed experimental investigations.

2.3.1. Multiple ionization in the intermediate regime. The ionization process induced by swift heavy ion collisions on atomic targets is certainly the process which provided the main motivation to develop the COLTRIMS technique at beginning of the 90's [113-115]. Indeed, the ultimate goal was to get access to the scattering angle of the projectile, and hopefully to the impact parameter. As for fast collisions, the projectile scattering angle is too small to be measured directly, the idea was to infer it from the high resolution measurement of the recoiling target momentum. As mentioned above, the three pioneering groups working on this high resolution technique were the IKF, Frankfurt, Germany (H. Schmidt-Böcking), KSU, Manhattan, Kansas (C.L. Cocke) and CIMAP, Caen, France (A. Cassimi). The first results obtained with this technique have appeared in 1994 and have already evidenced the role of the electrons on the momentum balance. Their momentum has been shown to balance nearly exactly the target ion momentum making fast ion ionization resemble to photoionization.

One of the first COLTRIMS experiment performed at GANIL was aiming at the determination of the momentum vector of recoiling Ar and He target atoms ionized by Xe^{44+} (6.7 MeV/A) impact. From the angle of emission and recoil velocity distributions of each recoil ion charge state q (q = 1 to 7 for argon ions, q = 1 and 2 for helium ions), it was deduced that the recoil ions are mostly emitted backward with respect to the projectile beam direction (figure 7). This behaviour has been attributed to the electrons which are mainly emitted in the forward direction and thus prove, in the case of single and multiple-ionization, the importance of the role played by the electrons in the momentum balance of such a collision. Moreover, such a backward recoil ion emission proves that the interaction between the projectile and the ejected electrons on one hand and the interaction between the projectile and the target on the other hand, may not be considered as independent. As a consequence it could be stated that the two body collision model underestimates the kinetic energy deposited on the target nucleus [116].

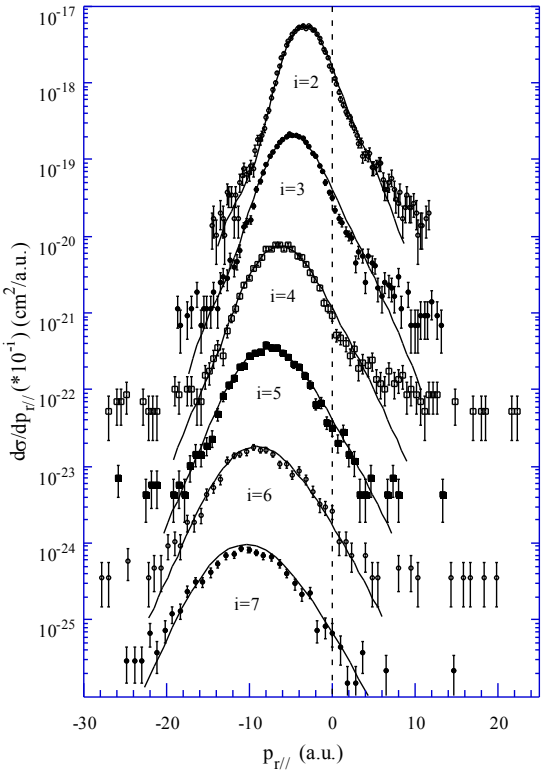

Figure 7. Experimental (dots) and calculated (lines) $d\sigma /dp_{r//}$ for Ar multiple ionization [116].

3. Collisions with diatomic species

3.1. Collisions with diatomic covalent molecules

3.1.1. Low energy collisions. Over the last decades, much work has been devoted to the study of slow collisions between highly charged ions and molecules [117-122]. Comparison between the collision time and the different molecular characteristic times (vibration, rotation) suggests a two-step picture for molecular fragmentation. In a first step, electron removal takes place on a fixed-in-space molecule and the transient molecular ion has the equilibrium internuclear distance of the neutral molecule. Then, in a second step, nuclear motion starts and is driven by the fragmentation dynamics. Pioneering calculations for the system $Xe^{54+} + H_2$ by means of the classical trajectory Monte Carlo method [123] suggested two main sources for the kinetic energy of each H^+ fragment: the recoil energy E_r induced by the projectile on the center of mass of the ionized target, and the fragmentation energy E_f due to a pure Coulombic dissociation. At high projectile velocities ($v_p \geq 0.5$ a.u.), the quantity E_r is negligible compared to E_f, so that the energy of the protons (~ 9.5 eV) originates only from the Coulomb explosion of the molecule at the Franck-Condon limit. In contrast, at low impact velocities ($v_p \leq 0.1$ a.u.), both slow and fast protons were predicted [123], resulting from the vector addition of the collisional momentum transfer to the center of mass of the molecule and the one due to the two-body Coulomb dissociation.

However, it has been recognized that a two-step picture is too simple [124-127]. Firstly, the fragmentation dynamics depends strongly on the primary electronic processes. In the case of multi-electron molecular targets, we have shown that electron capture can lead to the formation of inner-shell vacancies [128, 129], and thus to the excitation of the molecular target. By performing high-resolution kinetic-energy-release measurements on CO dissociation [125], the first experimental evidence that excitation of the molecular target affects the fragmentation dynamics has been provided, thus leading to significant deviations from the Coulomb explosion model. Secondly, the fragment ions may also be influenced by the outgoing projectile ion [124-127]. The influence of the projectile is similar to the well-known Post-Collision Interaction (PCI) which affects the energy spectra of Auger electrons emitted from a projectile in the field of an ionized target. The fragment energy shift due to this effect is expected to depend on the projectile charge, the projectile velocity and the orientation of the molecular target before the collision.

To get further insight into the post-collision interaction with the projectile, much effort has been devoted to investigate the fragmentation of H_2 in collisions involving O^{5+} and Xe^{23+} projectiles which strongly differ in charge, and occurring in a wide range of impact velocities (from 0.02 to 0.5 a.u.) [130, 131]. The energy distribution of the fragments was recorded at several angles with respect to the beam direction. The analysis of the spectra, combined with a classical scattering calculation, has shown that the projectile interacts strongly with each fragment. The lower the collision velocity, the lower the number of slow protons detected at forward angles ($< 90°$) [130, 131], since slow protons are repulsed in backward directions due to the Coulomb force induced by the projectile. Furthermore, at projectile velocities lower than 0.1 a.u., the energy distribution of the fragments exhibits two groups of peaks centered at energies which differ from the expected energy at the Franck-Condon limit ($E = 9.5$ eV): (*i*) slow fragments ($E \leq 10$ eV) are formed in soft collisions involving large impact parameters ($b > 1$ a.u.), while (*ii*) fast fragments originate from hard collisions between the projectile and one of the target protons [131]. This study provided the first experimental evidence that the relative contribution of hard collisions to double capture events increases when decreasing the projectile velocity [131]. We observed the same feature for electron capture following O^{5+} impact on an atomic target of helium [132], thus showing its generality.

At CIRIL, besides studies with the homonuclear H_2 target, investigations involving heteronuclear and multi-electron molecular species led to other important achievements and findings. For collisions of He^{2+} (11 keV/u) and O^{7+} (4 keV/u) on the CO molecule, the dependence of the capture process on the initial orientation of the molecule has been investigated by measuring in coincidence the full

momentum vector of the two fragments of the dissociated molecule and the projectile charge state [122]. In that study, the KER (Kinetic Energy Release) distribution for each fragmentation channel was obtained for each outgoing projectile charge state associated not only to single capture, but also to both stabilized and autoionizing double capture processes [122]. In the case of 98-keV N^{7+} + HCl collisions, peak structures in the energy distribution of H^+ fragments ejected from HCl molecules made possible the identification of excitation and multi-electron capture channels [133]. For collisions of 30-keV N^{6+} and O^{7+} ions with water and methane molecules, the angular distribution of the fragment ions revealed nucleus-nucleus binary collision effects, with the indication of an interplay between Coulomb explosion and binary collision mechanisms [134, 135]. An unexpected anisotropy has been found for the angular distribution of H^+ emission from water [134, 135], which could be attributed to orientation sensitivity of some of the capture channels [134-137].

More recently, it has been shown that negative hydrogen ions (H^-) can be formed in molecular collisions under much more general conditions than ever expected, via a previously unrecognized process [138, 139]. H^- formation has been observed in collisions between a positively-charged molecular ion (7-keV OH^+) and a neutral target (argon atom or acetone molecule). By measuring both energy and angular distributions of the emitted anions, it has been shown that H^- ions can be created via quasi-elastic two-body collisions involving a large momentum exchange between a heavy atomic center and the active H center. Hence, fragile atomic systems such as negative hydrogen ions are formed not only in soft collisions involving negligible momentum transfer, but also in hard core-core collisions via double electron grabbing by fast hydrogen fragments. For 7-keV OH^+ + Ar, a striking finding is that negative and positive hydrogen ions are emitted with very similar angular dependences [140]. Though the electron capture process is complex, the relative population of the different final charge states of the outgoing fragments can be described by simple statistical laws.

3.1.2. Medium and high energy collisions. The availability of new position sensitive detectors with the capability of multi-particle detection has opened the way to the study of the molecule fragmentation dynamics. The CIMAP has been one of the first laboratories to use this technique for the study of ion induced molecular fragmentation and took advantage of the quality GANIL ion beams [141]. As for COLTRIM spectroscopy, this imaging technique allows to measure momenta of all fragments becoming a multi-particle 4π spectrometer.

Opposite to ion-atom collisions, large momenta (up to 100 a.u.) are imparted to the molecular fragments. In this latter case, the momenta reflect the dynamics of the fragmentation process rather than the collision dynamics as it is the case for atomic targets. Indeed, they give access, with high resolution, to the Kinetic Energy Release (usually noted KER which is the sum of all fragments kinetic energy) allowing identification of the molecular excited states before the molecule dissociation. Figure 8 shows that, depending on the projectile velocity governing the dominant process (electron capture at low velocity and ionization at high velocity), the populated excited states of the CO dication are clearly different [142]. This was the first time that molecular excited states could be separated, proving the limit of the so called Coulomb explosion model which assumes that the KER is given by the Coulomb repulsion between the fragments starting at the neutral molecule atom position and holding their final charge state.

In the case of ion-molecule collisions, the target has a structure which adds new degrees of freedom such as the orientation of the molecule with regard to the beam direction. Dealing with fast projectile ions, the collision duration is much shorter (10^{-17} s) than the dissociation (10^{-14} s) and the rotation (10^{-11} s) times. This leads to two main features of this process:

- The atto-second interaction duration allows to study the free fragmentation process, without any influence of the projectile Coulomb field.
- As the rotation lasts longer than the fragmentation process, the fragment momenta keep memory of the molecule orientation at the instant of the interaction with the projectile which can thus be reconstructed.

These features have allowed to study the dependence of collision processes on the molecule orientation [141]. Strong effects have been observed and interpreted by geometric models [143, 144, 145, 146] evidencing that orientation effects become important for processes happening at impact parameters of the same order of the size of the target molecule such as inner-shell processes or multiple ionization.

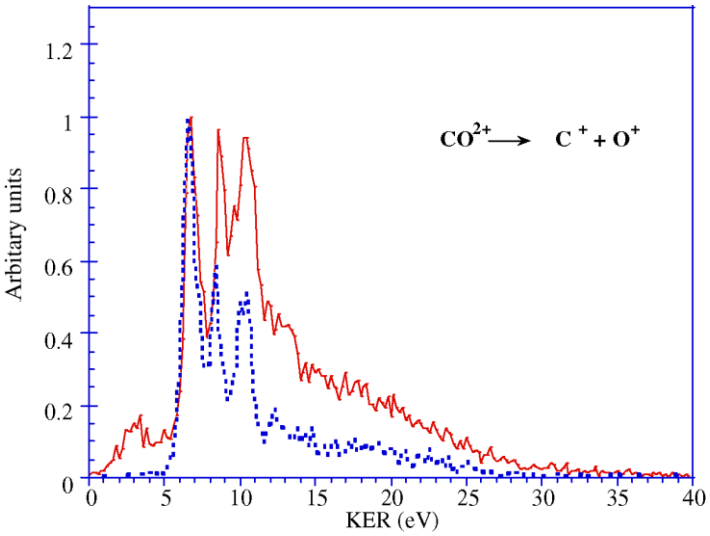

Figure 8. Comparison of the kinetic energy release distributions for the $C^+ + O^+$ fragmentation channel induced by 11.4 MeV u^{-1} O^{7+} (full curve) and 4 keV u^{-1} O^{7+} (dotted curve) projectiles [142].

When the target gets larger than diatomic molecules, the fragmentation dynamics starts to become more complex due to its many-body nature. Already for tri-atomic molecules such as CO_2, internal degrees of freedom increase the number of fragmentation scenarios entering into play, the fragmentation being either sequential or concerted [141]. This complicated dynamics has been accessible thanks to the latest multi-particle imaging techniques available at the end of the 90's. This dynamics can even lead to surprising isotopic effects such as those observed in the case of HDO molecules (figure 9) [147] for which the probability of losing the H^+ fragment is more than 5 times higher than for the D^+ fragment.

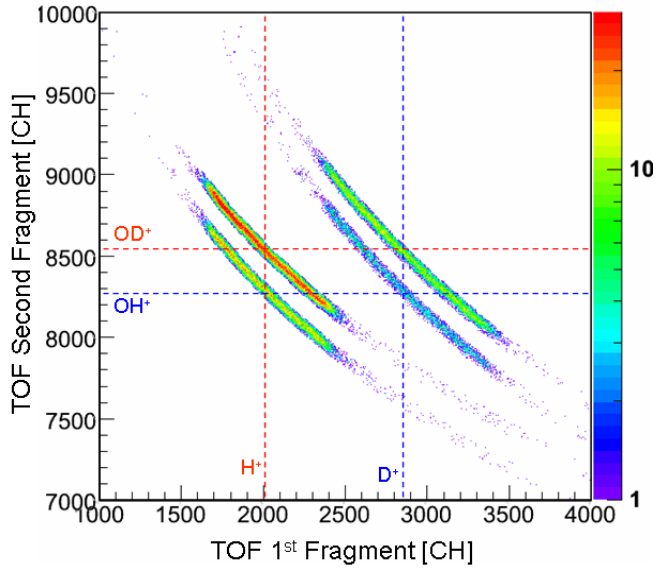

Figure 9. Two-body fragmentation channels of H_2O, D_2O and HDO mixture showing the the dominant $OD^+ + H^+$ fragmentation channel of the dication HDO^{2+} [148].

3.2. Collisions with rare gas dimers

Very recently, rare-gas dimer targets have attracted much attention. They are characterized by a large internuclear distance and a weak molecular bond, providing a situation where the target can behave more like two neighbor independent atoms than like a covalent molecule. Photoionization experiments have already shown that new deexcitation channels open up for an ion located in the vicinity of another atom [149,150]. The new relaxation process, called inter atomic Coulombic decay (ICD) and initially predicted by Cederbaum *et al* [151], has been observed for biologically relevant systems such as water clusters [152] and a vast number of rare-gas clusters [153]. This process is thus an additional source of low-energy electrons that can play a role in radiation damage to healthy tissues.

In this context, the contribution of ICD to the production of low-energy electrons induced by ion impact had to be investigated. In ionizing ion-atom collisions at medium and high energy collisions, the dominant contribution to the electron energy distribution results from distant collisions with small energy transfers which can be approximated by an exponential decay. Recent experiments performed at GANIL with 11.37 MeV/u S^{14+} ions colliding on neon dimers have shown a large contribution of low-energy electron production unambiguously attributed to ICD [154]. Combined with complementary experiments using He^{+} and He^{2+} projectiles in the 0.1-0.2 MeV/u energy range on neon and argon dimer targets, the results suggest that ICD is omnipresent and a major contributor of low-energy electron emission in fast ion collisions with loosely bound targets [154].

For lower energy collisions between HCIs (highly charged ions) and molecular targets, multiple electron capture becomes the dominant primary process. For molecular targets with a strong covalent character, for which the valence electronic orbitals are delocalized over the whole molecule, multiple ionization leads usually to dissociation into equally charged fragments [155-157]. With rare gas dimer targets, if one site of the dimer is multiply ionized, near isolation of the two atoms may lead to weaker and slower charge rearrangement. This unique feature may allow to investigate how the electrons are captured at the instant of the collision and to study electron dynamics in charge transfer collisions with HCIs. In an experiment involving low energy Ar^{9+} projectiles colliding on Ar_2, the yields associated to the different fragmentation channels $Ar^{+} + Ar^{+}$, $Ar^{2+} + Ar^{+}$, $Ar^{3+} + Ar^{+}$ and $Ar^{2+} + Ar^{2+}$ were precisely measured. In contrast with the results previously obtained with covalent molecules, it was shown that asymmetric fragmentation channels are favored [158,159]. In addition, the kinetic energy release (KER) spectrum of the $Ar^{+} + Ar^{+}$ fragmentation channel allowed to identify one-site double capture process populating bound transient states that can only decay through radiative charge transfer (RCT). This behavior was interpreted as due to low electron-mobility within the molecular ions resulting from the collision.

This finding motivated a more detailed study of the collision system with the measurement of the correlation between the projectile scattering angle and the molecular ion orientation, as a function of the fragmentation charge sharing. As illustrated in the figures 10.a and 10.b, the projectile scattering angle ϕ_{proj} is given by the transverse momentum exchange due to the Coulomb repulsion between the collision partners. It is thus closely related to the impact parameter vector $\vec{b}$ in the molecular frame and to the final charge on the two sites of the dimer. The experimental results provided clear evidence that projectiles distinguish each atom in the target and, that electron capture from near-site atom is favored [160]. Monte Carlo calculations based on the classical over-the-barrier model, with dimer targets represented as two independent atoms, were compared to the data. These calculations, in good agreement with the experimental data, give a new insight into the dynamics of the collision by providing, for the different electron capture channels, the two-dimensional probability maps $p(\vec{b})$ [160].

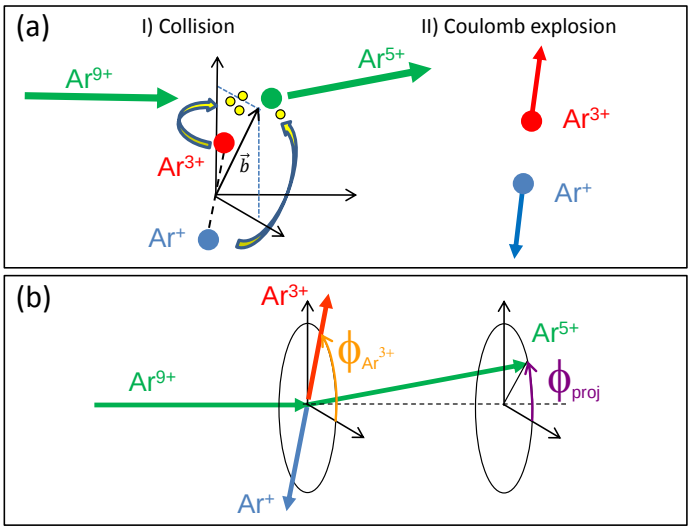

Figure 10. (Color online) Schematic view of the multiple electron capture from Ar_2 by Ar^{9+}projectiles resulting in the Ar^{3+}+ Ar^{+} asymmetric fragmentation channel (a). Representation of the scattering angle ϕ_{proj} and of the angle of emission ϕ_{Ar3+} of the most charged fragment in the plane transverse to the beam axis (b).

4. Probing other fundamental processes

4.1. Young-type interferences induced by ion-molecule collisions

Since 2001, many experiments have been devoted to the evidence for oscillations in angular distribution and energy distribution of electrons emitted in collisions of highly charged, fast and slow ions [161-178] and electrons [179] with H_2 molecules. First, structures attributed to interference effects in the electron emission spectra from H_2, which are similar to those observed in Young's two-slit experiment, were observed [161-166]. For ion-induced electron emission the interference structures were difficult to observe. Therefore theory has been used to provide guidance in the search for the interference phenomena. Fast projectiles have been found to be essential ($v > 10$ a.u.), since they enhance dipole-like transitions which, in turn, are responsible for the interference effects. Various features predicted by the model calculations are in accordance with the experimental results: (i) interference effects do not cancel when an averaging is performed over the orientation of the H_2 internuclear axis, (ii) interference effects are manifested by a sinusoidal-like oscillation occurring in an energy range up to 250 eV. Evidence is provided for the fact that the oscillation frequency of the interference pattern varies significantly with the electron ejection angle. The theoretical results based on Born approximation confirm this behavior. However, the theory cannot explain the high frequency observed at high emission angles [166].

A few years later, interferences caused by a single electron impacting on an independent double-center scatterer, which plays the role of an atomic-size double-slit system, were experimentally evidenced for the first time [167-178]. The electron originates from the autoionization of doubly excited $2lnl'$ ($n \geq 2$) configurations of He following a double charge exchange process by He^{2+} ions impinging on H_2 molecules. Well-defined oscillations could be observed in the angular distribution of the electrons emitted towards the receding H protons. The presence of these oscillations provides the first experimental demonstration that a single electron interferes with itself [167]. This is analogous to the famous "thought" experiment imagined and discussed by Feynman in 1963, in which the quantum nature of the electron was illustrated by making it traverse an atomic-size double-slit arrangement.

An interesting aspect of electron interferences was also evidenced [174]. Instead of investigating the total intensity of undiscerned $2lnl'$ ($n \geq 2$) autoionization configurations, focus has been put on a

single $2s^2\,{}^1S$ line. Its maximum and linewidth have been determined at angles ranging from 120° to 160°, where interferences are expected to occur. This detailed analysis revealed well-defined oscillations in the angular dependence of both the maximum intensity and the linewidth. In the investigated angular range, the maximum oscillates in phase with the total intensity, showing that the oscillations of the total intensity are mainly due to the variations of the line maximum. More surprisingly, the $2s^2\,{}^1S$ linewidth was found to strongly oscillate in counter phase with the maximum, a fact that can be explained by means of simple theoretical arguments. These results not only provide a Feynman-type demonstration of the presence of a nanoscale Young-type interference of single electrons but also complete and reinforce the analysis performed previously on the undiscerned $2lnl'$ ($n \geq 2$) configurations.

4.2. Electron shakeoff in nuclear beta decay

Electron shakeoff (SO) is a fundamental atomic process resulting from the sudden change of the central potential in which a bound electron is ejected into the continuum. This monopole ionization may be due to the creation of a vacancy in an atomic inner shell induced by collisions with charged particles (see section 2.3.) or by photoionization [180], but also to the change of the nucleus charge in nuclear reactions such as nuclear beta decay, nuclear electron capture, internal conversion and alpha decay [181]. If the ionization probabilities can usually be calculated in the framework of the sudden approximation (SA), the accuracy of the calculation depends on how fast is the potential change compared with the relaxation time of the electrons in the new core potential. Nuclear beta decay offers ideal conditions since the potential change occurs in less than 10^{-18}s, which is the transit time of the emitted beta particles through the orbital electron cloud. Calculations of SO probabilities following beta decay were first performed using hydrogen like wave functions [182], and later, using more sophisticated numerical self-consistent wave functions for many electrons atoms [183]. However, the comparison between experiments and calculations is usually difficult because of secondary processes such as Auger electron emission that contribute to the final charge state of the daughter ions. Even for the simplest case investigated so far, the beta decay of ^{6}He atoms, the theoretical double ionization probability was overestimated by almost one order of magnitude [184].

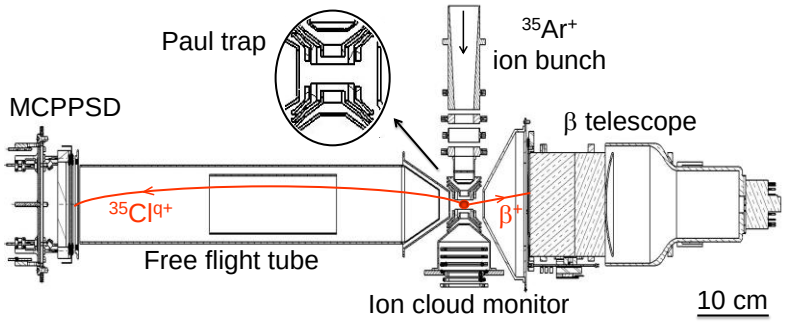

Figure 11. (Color online) Top view of the LPC trap setup and representation of a beta decay event from $^{35}Ar^+$ trapped ions. The recoiling daughter is accelerated between two collimators, enters a free flight region and is detected by a microchannel plate detector (MCPPSD). The detection of the beta particle provides a start for the recoil ion time of flight measurement, allowing charge state identification. The insert shows the structure of the Paul trap.

The LPC trap setup [185,186] has been initially developed to perform in-trap decay precision measurements [187] by confining radioactive ions from the SPIRAL target-ion source of GANIL in a transparent Paul trap. By implementing a new time-of-flight recoil ion spectrometer (figure 11) with the capability to separate the different charge states of the recoil ions resulting from beta decay, the setup has been recently used to investigate electron SO processes in the decay of singly charged radioactive ions. This new setup allowed, for the first time, to perform a SO measurement in the decay of $^6He^+$ ions. With only one single active electron, electron-electron correlations and secondary

relaxation processes are absent, leaving only two possible mechanisms for the daughter ionization: direct collision with the beta particle, and the rapid change of both, the nuclear charge and the recoil velocity of the daughter nucleus. In this ideal textbook case, the experimental ionization probability was measured with a relative precision of the order of 10^{-4} and the result, P_{SO}=0.02339(36), was found in perfect agreement with simple mechanical calculations based on the SA [188].

Beyond the prototypical $^{6}He^{+}$case, heavier systems such as $^{35}Ar^{+}$ can reveal the role of more subtle shakeoff dynamics involving several electrons, and of subsequent relaxation processes such as the emission of Auger electrons. A recent joined experimental/theoretical study of the SO process in $^{35}Ar^{+}$ decay has provided a quite complete picture of ion formation [189] showing, in particular, the importance of Auger electrons. The same technique will be applied to $^{19}Ne^{+}$ ions in order to get a Z-dependent picture of the underlying ionization mechanisms.

5. Conclusions and perspectives

We have presented in the previous sections a large panel of collision experiments performed at GANIL during the three last decades, in the field of ion-atom and ion-molecule interactions. Covering a wide range of collision regime, these experiments led to a better understanding for several fundamental issues such as, for example, the role of electron-electron interaction in double capture, the importance of multiple-capture or-ionization processes depending on the collision regime or the limits of the two-step picture in ion-molecule collisions. New relaxation channels have also been evidenced, in particular for multi-ionized rare gas dimer targets with the identification of the ICD and RCT processes, and for OH^{+} projectile ions leading unexpectedly to the formation of H^{-} ions. This experimental activity has given rise to several technological developments, such as the use of state-of-the-art X-ray spectrometers for the charge exchange process study, new spectrometers as well for the detection of molecular fragments, and the development of the recoil ion momentum spectroscopy technique. The quality and variety of the collected data have allowed testing and setting the limits of various theoretical models and calculations, such as the over-the-barrier model, the Landau-Zener model, CTMC calculations but also much more complex calculations such as close coupling based on atomic and molecular orbitals or two-center basis generator method. Beside the study of collisions, fundamental processes such as Young type interferences with a single electron or shakeoff ionization in nuclear beta decay are also part of the wide range of atomic physics topics that could be addressed at GANIL.

Most of these research topics are still very active, with a number of unanswered questions and a large place for new discoveries. We have seen that for medium and high energy collisions, the ICD process has a sizeable contribution in the emission of low energy electrons. This process can play an important role in radiation damage to biological tissues, and it is now necessary to extend its study to low energy collisions. Ion-molecule collisions have also been used as a tool to study Young type interferences with a single electron. Such collisions can be as well a powerful tool for molecular spectroscopy. As in the pioneering experiment performed with H_2^{+} ions [190], collision-induced fragmentation of exotic molecules such as “trilobite” Rb_2 molecules [191] could yield capital information on the internuclear distance and on the molecule vibrational states. For the shakeoff ionization induced by nuclear reactions, few experimental data are presently available. Experiments involving radioactive ions with a wider range of atomic numbers would complete the present picture for this process. Finally, the future installation SPIRAL2 should open up an entirely new experimental field: the investigation of ion collisions with very dilute targets. In particular, the very high intensity of the high-energy ion beams that will be delivered to the S^3 spectrometer, coupled to a dedicated low energy platform equipped with an ECR source, will enable to study ion-ion collisions in the unknown intermediate velocity regime but where nevertheless the energy deposition is optimum. Besides the possibility to reach “pure” 3-body systems (bare ions on hydrogenic targets) as a benchmark to test theory in the simplest case, we will explore the role of additional electrons, bounded either to the target and/or to the projectile –one by one- to quantify the effects of the N-body quantum dynamics.

This project [192], apart from its fundamental interest, is also of prime importance for applications since it should provide a real breakthrough in the understanding of energy transfers in various plasmas (stellar /interstellar or inertial confusion plasmas) and also in the description, at the atomic level, of material modifications, including biological materials.

Acknowledgments
We would like to deeply thank the GANIL and CIMAP staff from the machine and the different experimental areas who allowed the realization of these experiments which often required ion beams of high optic quality. We are very grateful to all the students and postdoctoral fellows, coming from different countries, who were strongly involved in the whole of the work presented here. We are also deeply thankful to our numerous collaborators from France and to the international community who initiated and contributed to many experiments at GANIL in the field of atomic and molecular physics during the last three decades.

References

[1] Bransden B H and McDowell M R 1992 *Charge Exchange and the Theory of Ion-Atom collisions* (Oxford)
[2] Cravens T E 2002 *Science* **296** 1042
[3] Isler R C 1994 *Plasma Phys. Contr. F.* **36** 171
[4] Uehara S, Toburen L and Nikjoo H 2001 *Int. J. Radiat. Biol.***77** 139
[5] Uehara S and Nikjoo H 2002 *J. Phys. Chem.* B **106** 11051
[6] Ryufuku H, Sasaki K and Watanabe T 1980 *Phys. Rev.* A **21** 745
[7] Boduch P, Chantepie M, Hennecart D, Husson X, Kucal H, Lecler D, and Lesteven-Vaïsse I 1989 *J. Phys.* B **22** L377
[8] Jacquet E, Boduch P, Chantepie M, Druetta M, Hennecart D, Husson X, Lecler D, Olson R, Pascale J and Wilson M 1993 *Phys. Scripta* **47** 618
[9] Cowan R D 1981 *The theory of atomic structure and spectra* (Berkley : University of California Press)
[10] Boduch P, Chantepie M, Druetta M, Fawcett B, Hennecart D, Husson X, Kucal H, Stolterfoht N and Wilson M 1992 *Phys. Scripta* **45** 203
[11] Bazin V, Boduch P, Chantepie M, Cremer G, Jacquet E, Kucal H, Lecler D and Pascale P 2000 *Phys. Rev.* A **62** 052706
[12] Bazin V, Boduch P, Chantepie M, Jacquet E, Kucal H, Lecler D and Pascale P 2002 *Phys. Rev.* A **65** 032712
[13] Laulhé C, Jacquet E, Boduch P, Chantepie M, Ghérardi N, Husson X, Lecler D and Pascale J 1997 *J. Phys.* B **30** 2899
[14] Abrines R and Percival I C 1966 *Proc. Phys. Soc. Lond.* **88** 861
[15] Olson RE and Salop A 1977 *Phys. Rev.* A **16** 531
[16] Jacquet E, Pascale J, Boduch P, Chantepie M and Lecler D 1995 *J. Phys.* B **28** 2221
[17] Jacquet E, Chantepie M, Boduch P, Laulhé C, Lecler D and Pascale P 1999 *J. Phys.* B **32** 1151
[18] Fano U and Macek J H 1973 *Rev. Mod. Phys.* **45** 553
[19] Lin C D and Macek J H 1987 *Phys. Rev.* A **35** 5005
[20] Laulhé C, Jacquet E, Cremer G, Pascale J, Boduch P, Rieger G, Chantepie M and Lecler D 1997 *Phys. Rev.* A **55** 1088
[21] Jardin P *et al* 1993 Recoil Ion Kinetics *AIP Conf. Proc.* **274** (1993, New York : AIP) p 291
[22] Ullrich J *et al* 1994 *Comments At. Mol. Phys.* **30** 235
[23] Cocke C L *et al* 1991 *Phys. Rep.* **205** 153
[24] Cederquist H, Biedermann C, Selberg N and Hvelplund P 1995 *Phys. Rev.* A **51** 2169
[25] Cassimi A, Duponchel S, Fléchard X, Jardin P, Sortais P, Hennecart D and Olson R E 1996 *Phys. Rev. Lett.* **76** 3679

[26] Duponchel S, Cassimi A, Fléchard X, Hennecart D, Adoui L, Jardin P, Sortais P and Olson R 1997 *Phys. Scripta* **73** 199
[27] Zhang H *et al* 1999 *Phys. Rev.* A **60**, 3694
[28] Fléchard X, Harel C, Jouin H, Pons B, Adoui L, Frémont F, Cassimi A and Hennecart D 2001 *J. Phys.* B **34** 2759
[29] Roncin P, Barat M, Laurent H, Pommier J, Dousson S and Hitz D 1984 *J. Phys.* B **17** L521
[30] Stolterfoht N, Havener C C, Phaneuf R A, Swenson J K, Shafroth S M and Meyer F W 1986 *Phys. Rev. Lett.* **57** 74
[31] Barat M, Gaboriaud M N, Guillemot L, Roncin P, Laurent H and Andriamonje S 1987 *J. Phys.* B **20** 5771
[32] Harel C and Jouin H 1990 *Europhys. Lett.* **11** 121
[33] Harel C, Jouin H and Pons B 1991 *J. Phys.* B **24** L425
[34] Roncin P, Gaboriaud M N and Barat M 1991 *Europhys. Lett.* **16** 551
[35] Martin S, Denis A, Delon A, Désesquelles J and Ouerdane Y 1993 *Phys. Rev.* A **48** 1171
[36] Martin S, Bernard J, Denis A, Désesquelles J, Chen Li and Ouerdane Y 1994 *Phys. Rev.* A **50** 2322
[37] Martin S, Bernard J, Chen Li, Denis A and Désesquelles J 1995 *Phys. Rev.* A **52** 1218
[38] Frémont F, Sommer K, Hicham S, Boduch P, Lecler D and Stolterfoht N 1992 *Phys. Rev.* A **46** 222
[39] Frémont F, Sommer K, Hicham S, Boduch P, Lecler D and Stolterfoht N 1993 *Nucl. Instrum. Meth.* B **79** 3
[40] Frémont F, Merabet H, Chesnel J Y, Husson X, Lepoutre A, Lecler D, Rieger G and Stolterfoht N 1994 *Phys. Rev.* A **50** 3117
[41] Chesnel J Y, Merabet H, Husson X, Frémont F, Lecler D, Jouin H, Harel C and Stolterfoht N 1996 *Phys. Rev.* A **53** 2337
[42] Merabet H, Cremer G, Frémont F, Chesnel J Y and Stolterfoht N 1996 *Phys. Rev.* A **54** 372
[43] Chesnel J Y, Merabet H, Frémont F, Cremer G, Husson X, Lecler D, Rieger G, Spieler A, Grether M and Stolterfoht N 1996 *Phys. Rev.* A **53** 4198
[44] Chesnel J Y, Sulik B, Merabet H, Bedouet C, Frémont F, Husson X, Grether M, Spieler A and Stolterfoht N 1998 *Phys. Rev.* A **57** 3546
[45] Frémont F, Bedouet C, Husson X, and Chesnel J Y 1998 *Phys. Rev.* A **57** 4379
[46] Chesnel J Y, Merabet H, Sulik B, Frémont F, Bedouet C, Husson X, Grether M and Stolterfoht N 1998 *Phys. Rev.* A **58** 2935
[47] Chesnel J Y, Frémont F, Sulik B, Ruiz-Méndez C, Merabet H, Bedouet C, Husson X, Grether M and Stolterfoht N 1999 *Nucl. Instrum. Meth.* B **154** 142
[48] Frémont F *et al* 2002 *Int. J. Mol. Sci.* **3** 115
[49] Fléchard X, Duponchel S, Adoui L, Cassimi A, Roncin P and Hennecart D 1997 *J. Phys.* B **30** 3697
[50] Moretto-Capelle P, Bordenave-Montesquieu D and Bordenave-Montesquieu A 1999 *Phys. Scripta* **1999** 118
[51] Sanchez I and Bachau H 1995 *J. Phys.* B **28** 795
[52] Kazansky A K and Roncin P 1994 *J. Phys.* B **27** 5537
[53] Frémont F, Bedouet C, Chesnel J Y, Merabet H, Husson X, Grether M, Spieler A and Stolterfoht N 1996 *Phys. Rev.* A **54** R4609
[54] Bedouet C *et al* N 1999 *Phys. Rev.* A **59** 4399
[55] Barat M and Roncin P, 1992 *J. Phys.* B **25** 2205
[56] Mack M, Nijland J H, Straten P v d, Niehaus A and Morgenstern R 1989 *Phys. Rev.* A **39** 3846
[57] Vernhet D, Chetioui A, Rozet J P, Stephan C, Wohrer K, Touati A, Politis M F, Bouisset P, Hitz D and Dousson S 1988 *J. Phys.* B **21** 3949

[58] Martin S, Denis A, Ouerdane Y, Salmoun A, El Motassadeq A, Désesquelles J, Druetta M, Church D, and Lamy T 1990 *Phys. Rev. Lett.* **64** 2633
[59] Chetioui A *et al* 1990 *J. Phys.* B **23** 3659
[60] Stolterfoht N, DuBois R D and Rivarola R D 1997 *Springer Series in Atomic, Optical, and Plasma Physics* vol 20 (Berlin : Springer)
[61] Currel F J 2003 *The Physics of Multiply and Highly Charged Ions: Interactions with Matter* vol 2 (Dordrecht : Kluwer)
[62] Janev R K and Winter H 1985 *Phys. Rep.* **117** 265
[63] Ryufuku H, Sasaki K and Watanabe T 1980 *Phys. Rev.* A **21** 745
[64] Taulbjerg K 1986 *J. Phys.* B **19** L367
[65] Fritsch W and Lin C D 1984 *Phys. Rev.* A **29** 3039
[66] Winter T G and Lin C D 1984 *Phys. Rev.* A **29** 567
[67] Kimura M and Lin C D 1987 *Comments At. Mol. Phys.* **20** 35
[68] Errea L F, Gomez-Llorente J M, Mendez L and Riera A 1987 *J. Phys.* B **20** 6089
[69] Barany A, Astner G, Cederquist H, Danared H, Huldt S, Hvelplund P, Johnson A, Knudsen H, Liljeby L and Rensfelt K G 1985 *Nucl. Instrum. Meth.* B **9** 397
[70] Ali R, Cocke C L, Raphaelian M L A and Stockli M 1994 *Phys. Rev.* A **49** 3586
[71] Zhang H *et al* 2001 *Phys. Rev.* A **64** 012715
[72] Selberg N, Biederman C and Cederquist H 1996 *Phys. Rev.* A **54** 4127
[73] Beiersdorfer P, Olson R E, Brown G V, Chen H, Harris C L, Neill P A, Schweikhard L, Utter S B and Widmann K 2000 *Phys. Rev. Lett.* **85** 5090
[74] Tawara H, Richard P, Safronova U I and Stancil P C 2001 *Phys. Rev.* A **64** 042712
[75] Tawara H, Takacs E, Suta T, Makonyi K, Ratliff L P and Gillaspy J D 2006 *Phys. Rev.* A **73** 012704
[76] Allen F I, Biedermann C, Radtke R, Fussmann G and Fritzsche S 2008 *Phys. Rev.* A **78** 032705
[77] Cravens T E 2002 *Science* **296** 1042
[78] Krasnopolsky V A, Greenwood J B and Stancil P C 2004 *Space Sci. Rev.* **113** 271
[79] Otranto S and Olson R E 2011 *Phys. Rev.* A **83** 032710
[80] Trassinelli M, Prigent C, Lamour E, Mezdari F, Mérot J, Reuschl R, Rozet J-P, Steydli S and Vernhet D 2012 *J. Phys.* B **45** 085202
[81] Salehzadeh A and Kirchner T, 2013, *J. Phys.* B **49** 025201
[82] Salehzadeh A, Trassinelli M, Prigent C, Lamour E, Rozet J-P, Steydli S, Vernhet D, and Kirchner T 2014 *J. Phys. Conf. Ser.* **488** 082006
[83] Bethe H A 1930 *Ann. Physics* (*Leipzig*) **5** 325
[84] Stolterfoht N 1991 *Nucl. Instrum. Meth.* B **53** 477
[85] Crasemann B 1989 *Comments At. Mol. Phys.* **22** 163
[86] McGuire J H, Berrah N, Bartlett R J, Samson J A R, Tanis J A, Cocke C L and Schlachter A S 1995 *J. Phys.* B **28** 913
[87] Skogvall B *et al* 1995 *Phys. Rev.* A **51** R4321
[88] Stolterfoht N *et al* 1998 *Phys. Rev. Lett.* **80** 4649
[89] Stolterfoht N *et al* 1999 *Phys. Rev.* A **59** 1262
[90] Stolterfoht N *et al* 2000 *AIP Conf. Proc.* **506** 427
[91] Tanis J A *et al* 1999 *Phys. Scripta* **T80** 381
[92] Tanis J A *et al* 1999 *Phys. Rev. Lett.* **83** 1131
[93] Tanis J A *et al* 2000 *Phys. Rev.* A **62** 032715
[94] Chesnel J Y *et al* 2002 *Photonic, Electronic and Atomic collisions* ed Burgdörfer J et al (*Rinton Press Princeton*) p 699
[95] Tanis J A *et al* 1998 *Phys. Rev.* A **57** R3154
[96] Rangama J, Hennecart D, Stolterfoht N, Tanis J A, Sulik B, Frémont F, Husson X and Chesnel J Y 2003 *Phys. Rev.* A **68** 040701(R)

[97] Bapat B *et al* 1999 *J. Phys.* B **32** 1859
[98] Schulz M *et al* 2001 *J. Phys.* B **34** L305
[99] Schulz M *et al* 2003 *Nature* **422** 48
[100] Lüdde H J *et al* 1995 *J. Phys.* B **28** 4101
[101] Kirchner T, Lüdde H J, Hortabsch M 2004 *Phys. Scripta* **T110** 364
[102] Montenegro E C, Meyerhoff W E, McGuire J H 1994 *Adv. Atom. Mol. Opt. Phys.* **34** 249
[103] Montenegro E C, Santos A C F, Melo W S, Sant'Anna M M and Sigaud G M 2001 *Phys. Rev. Lett.* **88** 013201
[104] Montanari C, Miraglia J E, Arista N R 2003 *Phys. Rev.* A **67** 062702
[105] Kirchner T et al 2005 *Phys. Rev.* A **72** 012707
[106] Monti J M *et al* 2011 *J. Phys.* B **44** 195206
[107] Fregenal D *et al* 2014 *J. Phys. Conf. Ser.* **488** 082014
[108] Chabot M *et al* 1994 *J. Phys.* B **27**, 111
[109] Adoui L *et al* 1994 *Nucl. Instrum. Meth.* B **87**, 45
[110] Adoui L *et al* 1994 *Nucl. Instrum. Meth.* B **98**, 312
[111] Vernhet D *et al* 1996 *Nucl.Instrum. Meth.* B **107**, 71
[112] Vernhet D *et al* 1997 *Phys. Rev. Lett.* **83** 1131
[113] Ullrich J *et al* 2000 *J. Phys.* B **30** 2917
[114] Dörner R *et al* 2000 *Phys. Rep.* **330** 95
[115] Cassimi A 1999 *Phys. Scripta* **T80** 98
[116] Jardin P *et al* 1996 *Nucl.Instrum. Meth.* B **107** 41
[117] Shah M B and Gilbody H B 1990 *J. Phys.* B **23** 1491
[118] McLaughlin T K, McCullough R W and Gilbody H B 1992 *J. Phys.* B **25** 1257
[119] Meng L, Olson R E, Folkerts H O and Hoekstra R 1994 *J. Phys.* B . **27** 2269
[120] Folkerts H O, Hoekstra R and Morgenstern R 1996 *Phys. Rev. Lett.***77** 3339
[121] Ben-Itzhak I, Wells E, Stöckli M P, Tawara H and Carnes K D 1997 *Phys. Scripta* **T73** 270
[122] Tarisien M, Adoui L, Frémont F and Cassimi A 1999 *Phys. Scripta* **T80** 182
[123] Wood C J and Olson R E 1999 *Phys. Rev.* A **59** 1317
[124] DuBois R D, Ali I, Cocke C L, Feeler C R and Olson R E 2000 *Phys. Rev.* A **62** 060701R
[125] Tarisien M *et al* 2000 *J. Phys.* B **33** L11
[126] Frémont F, Bedouet C, Tarisien M, Adoui L, Cassimi A, Dubois A, Chesnel J Y and Husson X 2000 *J. Phys.* B **33**, L249
[127] Adoui L *et al* 2001 *Phys. Scripta* **T92** 89
[128] Frémont F, Bedouet C, Husson X, Chesnel J Y and Stolterfoht N 1999 *Phys. Rev.* A **60** 3727
[129] Sobocinski P, Rangama J, Chesnel J Y, Tarisien M, Adoui L, Cassimi A, Husson X and Frémont F 2001 *J. Phys.* B **34** L367
[130] Sobocinski P, Rangama J, Chesnel J Y, Tarisien M, Adoui L, Cassimi A, Husson X and Frémont F 2001 *AIP Conf. Proc.* **576** 114
[131] Sobocinski P, Rangama J, Laurent G, Adoui L, Cassimi A, Chesnel J Y, Dubois A, Hennecart D, Husson X and Frémont F 2002 *J. Phys.* B **35** 1353
[132] Sobocinski P *et al* 2003 *J. Phys.* B **36** 1283
[133] Frémont F, Martina D, Kamalou O, Sobocinski P, Chesnel J Y, McNab I R and Bennett F R 2005 *Phys. Rev.* A **71** 042706
[134] Juhász Z, Chesnel J Y, Frémont F, Hajaji A and Sulik B 2008 *AIP Conf. Proc.* **1080** 118
[135] Juhász Z, Sulik B, Frémont F, Hajaji A and Chesnel J Y 2009 *Nucl. Instrum. Meth.* B **267** 326
[136] Sobocinski P, Pešić Z D, Stolterfoht N,Sulik B, Legendre S and Chesnel J Y 2005 *J. Phys.* B **38** 2495
[137] Sobocinski P, Pešić Z D, Hellhammer R, Klein D,Sulik B, Chesnel J Y and Stolterfoht N 2006 *J. Phys.* B **39** 927

[138] Juhász Z, Frankland B S, Frémont F, Rangama J, Chesnel J Y and Sulik B 2012 *J. Phys. Conf. Ser.* **388** 102051
[139] Juhász Z, Sulik B, Rangama J, Bene E, Sorgunlu-Frankland B, Frémont F and Chesnel J Y 2013 *Phys. Rev.* A **87** 032718
[140] Lattouf E *et al* 2014 *Phys. Rev.* A **89** 062721
[141] Cassimi A *et al* 2003 Many-particle quantum dynamics in atomic and molecular fragmentation *Atomic, Optical and Plasma Physics* (Springer-Verlag Berlin Heidelberg New-York) ed J Ullrich and V P Shevelko pp 1615-565
[142] Tarisien M *et al* 2000 *J. Phys.* B **33** L11
[143] Wohrer K and Watson R L 1993 *Phys. Rev.* A **48** 4784
[144] Caraby C, Cassimi A, Adoui L and Grandin J P 1997 *Phys. Rev.* A **55** 2450
[145] Kabachnik N M, Kondratyev V N, Roller-Lutz Z and Lutz H O 1998 *Phys. Rev.* A **57** 990
[146] Kabachnik N M, Kondratyev V N, Roller-Lutz Z and Lutz H O 1997 *Phys. Rev.* A **56** 2848
[147] Legendre S *et al 2005 J. Phys.* B **38** L233
[148] Muranaka T 2007 PhD thesis Univeisté de Caen Basse-Normandie
[149] Morishita Y *et al* 2006 *Phys. Rev. Lett.* **96** 243402
[150] Havermeier *T et al* 2010 *Phys. Rev. Lett.* **104** 133401
[151] Cederbaum L S, Zobeley J and Tarantelli F 1997 *Phys. Rev. Lett.* **79** 4778
[152] Jahnke T *et al* 2010 *Nature Phys.* **6** 139
[153] Averbukh V *et al* 2011 *J. Electron Spectrosc.* **183** 36
[154] Kim H K *et al* 2013 *Phys. Rev.* A **88** 042707
[155] Ben-Itzhak I, Ginther S G and Carnes K D 1993 *Phys. Rev.* A **47** 2827
[156] Wohrer K, Sampoll G, Watson R L, Chabot M, Heber O and Horvat V 1992 *Phys. Rev.* A **46** 3929
[157] Remscheid A, Huber B A, Pykavyj M, Staemmler V and Wiesemann K 1996 *J. Phys.* B **29** 515
[158] Matsumoto J *et al* 2010 *Phys. Rev. Lett*. **105** 263202
[159] Matsumoto J *et a*l 2011 *Phys. Scripta* **T144** 014016
[160] Iskandar W *et al* 2014 *Phys. Rev. Lett.* **113** 143201
[161] Stolterfoht N *et al* 2001 *Phys. Rev. Lett*. **87** 023201
[162] Stolterfoht N *et al* 2003 *Phys. Rev*. A **67** 030702R
[163] Stolterfoht N, Sulik B, Skogvall B, Chesnel J Y, Frémont F, Hennecart D, Cassimi A, Adoui L, Hossain S, and Tanis J A 2004 *Phys. Rev*. A **69** 012701
[164] Sulik B, Tanis J A, Chesnel J Y and Stolterfoht N 2004 *Phys. Scripta* **T110** 345
[165] Frémont F Hajaji A, Naja A, Leclercq C, Soret J, Tanis J A, Sulik B, Chesnel J Y 2005 *Phys. Rev.* A **72** 050704
[166] Tanis J A, Chesnel J Y, Sulik B, Skogvall B, Sobocinski P, Cassimi A, Grandin J P, Adoui L, Hennecart D, and Stolterfoht N 2006 *Phys. Rev*. A **74** 022707
[167] Chesnel J Y,Hajaji A, Barrachina R O and Frémont F 2007 *Phys. Rev. Lett*. **98** 100403
[168] Chesnel J Y,Hajaji A, Barrachina R O and Frémont F 2007 *J. Phys. Conf. Ser.* **58** 185
[169] Frémont F, Hajaji A, Barrachina R O and Chesnel J Y 2007 *J. Phys. Conf. Ser.* **88** 012020
[170] Frémont F, Hajaji A, Barrachina R O and Chesnel J Y 2007 *Reflets de la Physique, Journal SFP* **10** 10
[171] Frémont F, Hajaji A, Barrachina R O and Chesnel J Y 2008 *CR Phys.* **9** 469
[172] Frémont F, Suarez S, Barrachina R O, Hajaji A, Sisourat N, Dubois A and Chesnel J Y 2009 *Nucl. Instrum. Meth.* B **267** 206
[173] Frémont F, Gruyer D, Helaine V, Fossez K, Leredde A, Maclot S, Lepailleur A, Hajaji A, Chesnel J Y, Barrachina R O and S. Suárez 2009 *Handbook of Interferometers; Research, Technology and Applications* (Nova Science Publishers, Hauppauge, NY) ed D Halsey and W Raynor

[174] Barrachina R O, Frémont F, Fossez K, Gruyer D, Helaine V, Lepailleur A, Leredde A, Maclot S, Scamps G, and Chesnel J Y 2010 *Phys. Rev.* A **81** 060702R
[175] Frankland B, Barrachina R O, Chesnel J Y, Frémont F 2012 *J. Phys. Conf. Ser.* **388** 102009
[176] Vabre M, Girard S, Gilles H, Frankland B S, Porée F, Leprince P, Chesnel J Y, Barrachina R O, and Frémont 2012 *ISRN Spectroscopy* **2012** 174952
[177] Frémont F 2012 *Interférences électroniques Physique atomique - Interférences macroscopiques et nanoscopiques- Analogies avec les interférences photoniques* (Ellipses, Technosup, 2012)
[178] Frémont F 2013 *Springer Series on Atomic, Optical, and Plasma Physics* vol 77 (Springer, 2013)
[179] Kamalou O, Chesnel J Y, Martina D, J. Hanssen, Stia CR, Fojón O A, Rivarola R D, and Frémont F 2005 *Phys. Rev.* A **71** 010702R
[180] Wehlitz R, Heiser F, Hemmers O, Langer B, Menzel A and Becker U 1991 *Phys. Rev. Lett.* **67** 3764
[181] Freedman M 1974 *Annu. Rev. Nucl. Sci.* **24** 209
[182] Levinger JS 1953 *Phys. Rev.* **90** 11
[183] Carlson T A, Nestor C W, and Tucker J C 1968 *Phys. Rev.* **69** 27
[184] Wauters L and Vaeck N 1996 *Phys. Rev. C* **53** 497
[185] Fléchard X *et al* 2008 *Phys. Rev. Lett.* **101** 212504
[186] Rodriguez D *et al* 2006 *Nucl. Instrum. Meth.* A **565** 876
[187] Fléchard X *et al* 2011 *J. Phys.* G **38** 055101
[188] Couratin *C et al* 2012 *Phys. Rev. Lett.* **108** 243201
[189] Couratin *C et al* 2013 *Phys. Rev.* A **88** 041403 R
[190] Shmidt L Ph H, Jahnke T, Czasch A, Schöffler M, Schmidt-Böcking H and Dörner R 2012 *Phys. Rev. Lett.* **108** 073202
[191] Greene C H, Dickinson A S and Sadeghpour H R 2000 *Phys. Rev. Lett.* **85** 2458
[192] *http://www.insp.jussieu.fr/Collisions-Ion-Lent-Ion-Rapide.html*